A STUDY OF PALEOCLIMATES AS REFLECTED IN THE MASS ACCUMULATION RATE OF ICE-RAFTED DEBRIS RECOVERED FROM ODP LEG 152, SITE 918

by

Jessica Albrecht

A thesis submitted in partial fulfillment
of the requirements for the degree of

Bachelor of Science in Geological Sciences

The Ohio State University

1998

Approved by Lawrence Krissek
Dr. Lawrence A. Krissek

Abstract

Glaciomarine sediments recently recovered from the Irminger Basin provide the first available long-term record of ice-rafting activity along the southeastern Greenland margin, from the Pleistocene through the late Miocene. Ice-rafted debris mass accumulation rates (IRD MARs) of coarse (250 μm to 2 mm) terrigenous material in the Irminger Basin were investigated for the last 1.40 My (early Pleistocene). Intensification in IRD MAR peaks throughout the mid-Pleistocene appears to indicate at least a regional change in the history of glaciation along the SE coast of Greenland. Observations made in this study—particularly at 880 Ka—are consistent with the proposal of a mid Pleistocene climate shift in paleoclimatic records.

Acknowledgments

I would like to extend my sincere thanks to everyone who has supported me during this project. Special thanks go to my thesis advisor, Dr. Lawrence Krissek, for his continuous encouragement, sound advice, and helpful suggestions. He made this a pleasurable endeavor. I would also like to thank Kristen Kudless for providing her geological expertise, resources, and comprehensive support.

Many thanks go to my friends and colleagues for their encouragement and assistance. All have been invaluable to the completion of this thesis.

TABLE OF CONTENTS

LIST OF FIGURES

Introduction

This paper provides data that supplements an ice-rafting record previously generated by Kristen E. Kudless. The ultimate goal of this work is to understand the late Cenozoic glacial history of the Northern Hemisphere by interpreting paleoclimates as reflected in the mass accumulation rate (MAR) of ice-rafted debris (IRD). Information has been collected from Ocean Drilling Program (ODP) Leg 152 Site 918, which was located in the Irminger Basin off the SE coast of Greenland.

IRD is a direct indicator of the presence of glacial ice extending to sea level on adjacent landmasses. The sediments in this investigation are then studied:

–to determine the input of IRD by ascertaining the accumulation rates of these sediments over time;

–to compare these data to marine and continental records investigated in previous studies in order to derive a paleoclimatic signal from the mid-to-high latitudes;

–to determine if this region is a key nucleation area for widespread late Cenozoic glaciation.

Study Area

1. Setting

Site 918 is located in 1865.5 m of water on the upper continental rise off southeast Greenland within the western part of the Irminger Basin (Figure 1) (Larsen, 1994). The inner to mid-shelf is floored by Precambrian basement rocks that have a thin Quaternary cover (Figure 2). The outer shelf is floored by the landward edge of the SE Greenland Seaward Dipping Reflector Sequence (SDRS), which is covered by up to 1.5 km of Paleogene and Neogene sediments (Larsen, 1994). The SDRS continues under the slope and continental rise. The basement is covered here by at least 550 m of sediment (Larsen, 1994).

2. Lithostratigraphy

Site 918 is located on the upper continental rise, approximately 130 km east of the SE Greenland coast (Larsen, 1994). Complete descriptions of the Lithologic Units recovered at Site 918 are given by Shipboard Scientific Party (1994), therefore only a brief summary and a stratigraphic column (Figure 3) are provided here. The samples for this study are taken from Lithologic Unit 1, which extends from 0.0 to 600.0 mbsf (Holocene-late Miocene) and is dominated by dark gray silt. It is divided into five subunits, based upon the presence of graded beds in the upper two subunits. The lower three subunits are not covered in the

samples from this study, but note that Subunit 1C contains the highest concentration of IRD in Unit 1 (Shipboard Scientific Party, 1994). The base of Subunit 1D is marked by the last occurrence of an unequivocal in-situ dropstone at 543.6 mbsf (Shipboard Scientific Party, 1994). No dropstones were observed in Subunit 1E during the shipboard description (Shipboard Scientific Party, 1994). The upper 500 m of sediment contains abundant silts and mud, with numerous, typically granule- to pebble-size gravel clasts (Shipboard Scientific Party, 1994). A number of more massive beds, consisting of poorly sorted, ungraded silt, sand, and angular gravel, are also present (Shipboard Scientific Party, 1994).

Materials and Methods

The location of Site 918 is shown in Figure 1. This site was chosen for study because sediments recovered at Site 918 provided the first long-term ice-rafting record for this region—a possible key nucleation area for widespread late Cenozoic glaciation. The samples from this site have been studied for several parameters including:

–IRD MAR (Larsen, 1994; Kudless, in preparation)

–subpolar planktic and benthic foraminifers (Larsen, 1994; Nemoto, in press; Spezzaferri, in press)

1. Sample Size and Spacing

Samples 10 to 20 cc in volume originally were taken for studies by K.E. Kudless. Spacing of those samples was approximately 50 to 75 cm, from the Upper Miocene to Recent sediments of Hole 918A. Samples for this study were taken (as necessary) to fill in temporal gaps in the IRD MAR record already developed by K.E. Kudless.

2. Methods of Obtaining Data

Samples were dried at 60°C, weighed, disaggregated ultrasonically, and wet-sieved at 2 mm and 250 μm. The 2 mm to 250 μm fraction of each sample was dried at 60°C and weighed, and the abundance of the coarse-sand fraction was then calculated as a weight percent. The coarse-sand fraction of each of these samples was next examined with a hand lens to determine the abundance of terrigenous, non-volcanic material (the IRD) within the total coarse-sand fraction. In other studies, samples have been examined by binocular microscope to determine what other steps were needed (if any) to isolate the IRD from volcanic and biogenic coarse-grained components. In this study, however, examination with a hand lens was considered sufficient for identifying the coarse-fraction components. Volcanic ash was not a significant component in the

coarse-sand fraction, and therefore, physical separation of the ash from the rest of the coarse-sand fraction by means of heavy liquid techniques was not required.

In this study, mass accumulation rates, rather than IRD abundance (weight percent), are used as the indicator of the importance of IRD supply because IRD MARs are independent of the supply rates of other coarse-sand size components such as volcanic ash and biogenic material. The MAR of the coarse-sand sized IRD was calculated as,

$$\text{IRD MAR} = \text{CS \%} \times \text{IRD \%} \times \text{DBD} \times \text{LSR},$$

where IRD MAR is the mass accumulation rate ($g/cm^2/k.y.$), CS % is the coarse-sand abundance (weight %), IRD % is the abundance of IRD within the total coarse-sand fraction (weight %), DBD is the dry-bulk density of the sediment (g/cm3), and LSR is the linear sedimentation rate (cm/k.y.). All values used for these calculations are tabulated in Appendix I. Dry-bulk density values were obtained from tables of discrete shipboard physical properties measurements in Shipboard Scientific Party (1994). The stratigraphically closest discrete dry-bulk density measurement was used for each sample. LSRs were determined by K.E. Kudless as described below in Section 3.

3. Magnetostratigraphic and Biostratigraphic Age-depth Data

Magnetostratigraphic and biostratigraphic data were obtained from Shipboard Party (1994) and Nemoto (in press). These data were used as datums to determine the LSR for these samples. Micropaleontological studies of foraminifers were used as indicators of relative paleoclimates as well as for the aforementioned datums for the LSR calculation. These datums and the LSRs subsequently calculated are tabulated in Kudless (in preparation). Biostratigraphic data on the appearance and disappearance of species of foraminifers given by Nemoto (in press) are inconclusive to this study regarding paleoclimate. However, based upon dates obtained from foraminifers, the oldest samples analyzed here are dated as early Pleistocene (~1.40 Ma) and were taken from the upper ~76 m of Lithologic Unit 1.

Results

IRD abundances and MARs for each sample are tabulated in Appendix I. IRD abundance (weight %) is plotted versus depth downcore in Figure 4, and versus calculated age in Figure 5. Figure 6 is a plot of IRD MAR versus calculated age.

Interpretations

The oldest occurrence of significant IRD in this data set is dated at ~1.4 Ma, recording early Pleistocene ice-rafting off SE Greenland. A second early Pleistocene peak at 1.40 Ma is followed by a series of large peaks throughout the Pleistocene. The cause of these large pulses of Pleistocene ice-rafting is unknown, but the peaks may record important shifts in circulation, such as the position of the polar (melting) front and/or the influx of relatively warm North Atlantic water to the Norwegian-Greenland Sea during Pleistocene warming intervals. These abundance peaks may also be recording local surge events of SE Greenland tidewater glaciers. There also appears to be a gradual decrease in average peak size over the last ~300 Ka. This is consistent with what K.E. Kudless (in preparation) has found. This may have resulted from changes in ocean circulation such that the locus of iceberg melting no longer resided over this area, or from an overall decrease in iceberg melting from East Greenland glaciers (Kudless, in preparation).

Although there appears to be a gradual decrease in average peak size in the last ~300 Ka, there is an increase in the average MAR in samples younger than 880 Ka, in which peaks occur more frequently and the baseline MAR appears to increase. This mid-Pleistocene intensification in peak sizes appears to record at least a regional change, as it has also been observed in IRD records from the NW Pacific (Krissek *et al.*, 1985) and from the Norwegian Sea (Krissek, 1989). In addition, the mid-Pleistocene intensification of IRD MARs at this site—

specifically at 880 Ka—may be accompanied by changes in the period of apparent cyclicity in peak occurrence (i.e., the interval of repetition). Such observations are consistent with the proposal of a "mid-Pleistocene Revolution" (Fronval *et al.*, 1996; Mudelsee *et al.*, 1997) in paleoclimatic records.

For the purpose of this paper, the method I used to calculate the periodicity of IRD MAR peaks was sufficient. By using an IRD MAR value of 0.10 g/cm2/k.y. as the baseline for defining a "peak"—approximately the average MAR for the entire record—and counting the number of peaks in MAR abundance prior to and after the mid-Pleistocene shift (at ~880 k.y. in this study) a periodicity was calculated. There appears to be what may be interpreted as a periodicity of 50 Ka at an age of 0-700 Ka and 100 Ka at an age of 900-1400 Ka.

Mudelsee and Statteggar (1977) and Mudelsee and Schulz (1977) have found a 'dominant' cycle of 100 Ka after the mid-Pleistocene climate transition, and ~77 Ka prior to the mid-Pleistocene shift. While the cycles calculated by Mudelsee et al (1977) differ from the cycles determined in this study, the methods used to calculate the periodicities are quite different. Three main methods of time-series anlysis have been employed by others, including time-dependent mean and standard deviation, evolutionary spectral analysis, and time-dependent probability density function (Mudelsee *et al*, 1977). Artificial time series was applied by Mudelsee et al (1977) to benthic oxygen 18 isotope records. This in turn is interpreted as an indicator of mid-Pleistocene change in that there has been a multiple transition from a more linear climate system to a strong non-linear system.

In summary, the results obtained from this study help to understand the history of late Cenozoic glaciation in the Northern Hemisphere by determining peleoclimates as reflected in the mass accumulation rates of ice-rafted debris. Intensification of MAR peaks in the late Pleistocene and the appearance of a shift in the cyclicity of MARs are also helpful in interpreting the evidence for a mid-Pleistocene climate transition.

References Cited

Krissek, L.A., Morley, J.J., and Lofland, D.K., 1985. The occurrence, abundance, and composition of ice-rafted debris in sediments from DSDP sites 579 and 580, Northwest Pacific, *In* Heath, G.R., Burkle, L.H., et al., *Init. Repts. DSDP 86*:647-655.

Krissek, L.A., 1989. Late Cenozoic records of ice-rafting at ODP sites 642, 643, and 644, Norwegian Sea: Onset, chronology, and characteristics of glacial/interglacial fluctuations. *In* Eldholm, O., Thiede, J., Taylor, E., et al., *Proceedings of the Ocean Drilling Program, Scientific Results,* 145: 61-74.

Kudless, K.E., (in preparation). Temporal patterns in ice-rafting off SE Greenland: Miocene onset, Pliocene peaks, and Pleistocene correlations. *Ph.D. dissertation,* the Ohio State University.

Larsen, H.C., Saunders, A.D., and Clift, P.D., et al., 1994. Seven Million Years of Glaciation in Greenland. *Science* 264: 952-955.

Larsen, H.C., Saunders, A.D., and Clift, P.D., et al., 1994. *Proc. ODP, Init. Repts.,* 152, College Station, TX (Ocean Drilling Program).

Nemoto, N., (in press). Faunal changes of Neogene benthic foraminifers in the Irminger Basin. *ODP Leg 152 Sci. Results Volume.*

Shipboard Scientific Party, 1994. *In* Larsen, H.C., Saunders, A.D., and Clift, P.D., et al., *Proc. ODP, Init. Repts.,* 152, College Station, TX (Ocean Drilling Program).

Spezzaferri, S., (in press). Planktonic foraminifer biostratigraphy and paloenvironmental implications of Leg 152 Sites (East Greenland Margin). *ODP Leg 152 Sci. Results Volume.*

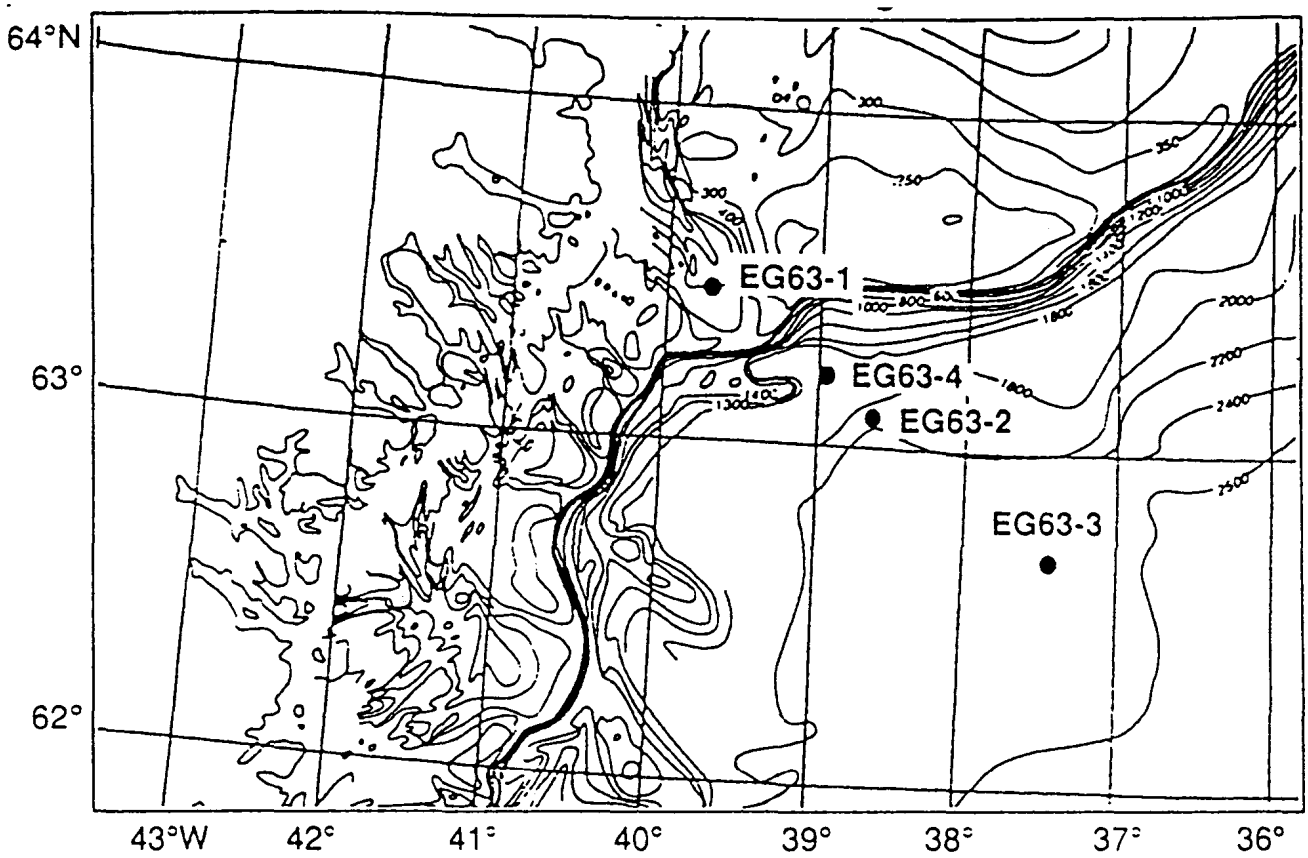

Figure 1.

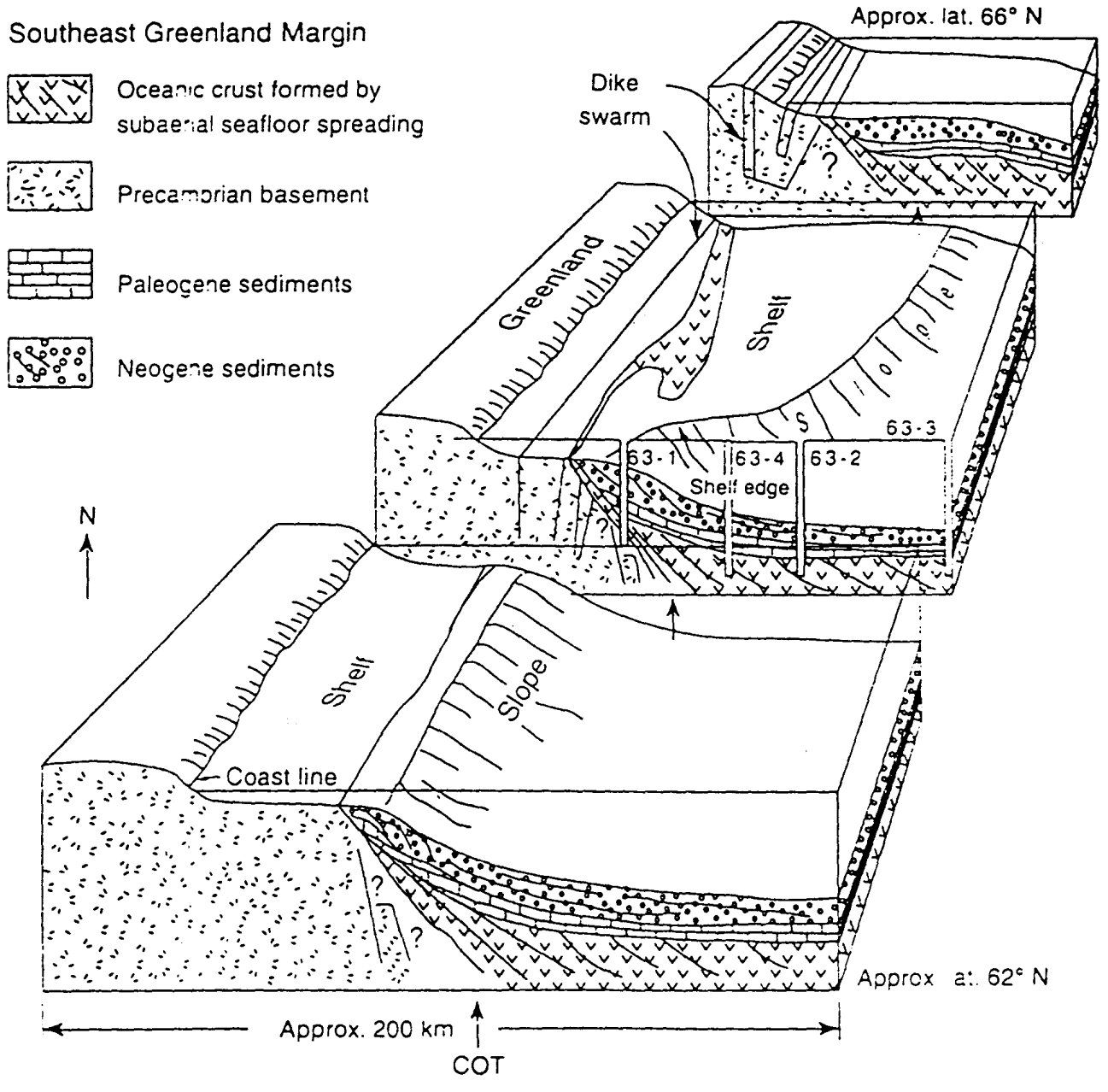
Southeast Greenland Margin
Oceanic crust formed by subaerial seafloor spreading
Precambrian basement
Paleogene sediments
Neogene sediments
Approx. lat. 66° N
Dike swarm
Greenland
Shelf
63-3
63-1
63-4
63-2
Shelf edge
N
Shelf
Slope
Coast line
Approx. lat. 62° N
Approx. 200 km
COT

Figure 2.

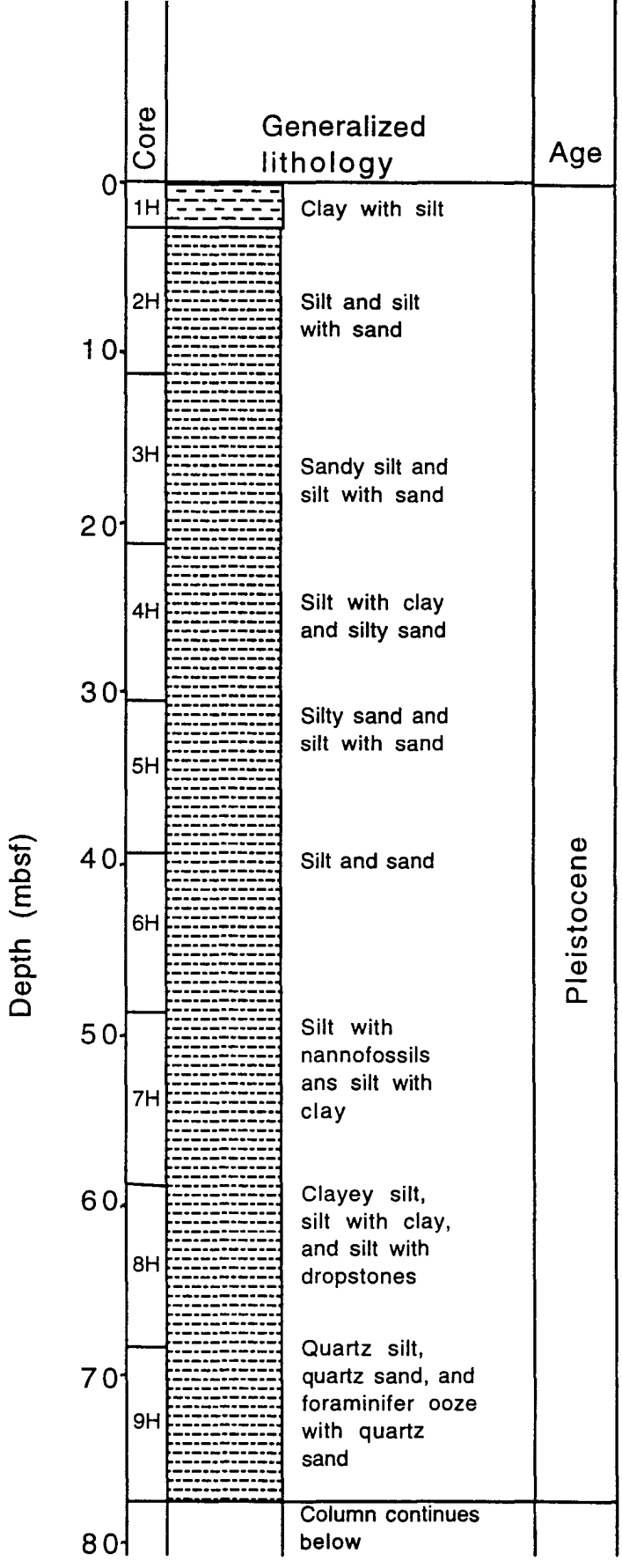
Core
Generalized lithology
Age
Depth (mbsf)
0
10
20
30
40
50
60
70
80
1H
2H
3H
4H
5H
6H
7H
8H
9H
Clay with silt
Silt and silt with sand
Sandy silt and silt with sand
Silt with clay and silty sand
Silty sand and silt with sand
Silt and sand
Silt with nannofossils ans silt with clay
Clayey silt, silt with clay, and silt with dropstones
Quartz silt, quartz sand, and foraminifer ooze with quartz sand
Column continues below
Pleistocene

Figure 3.

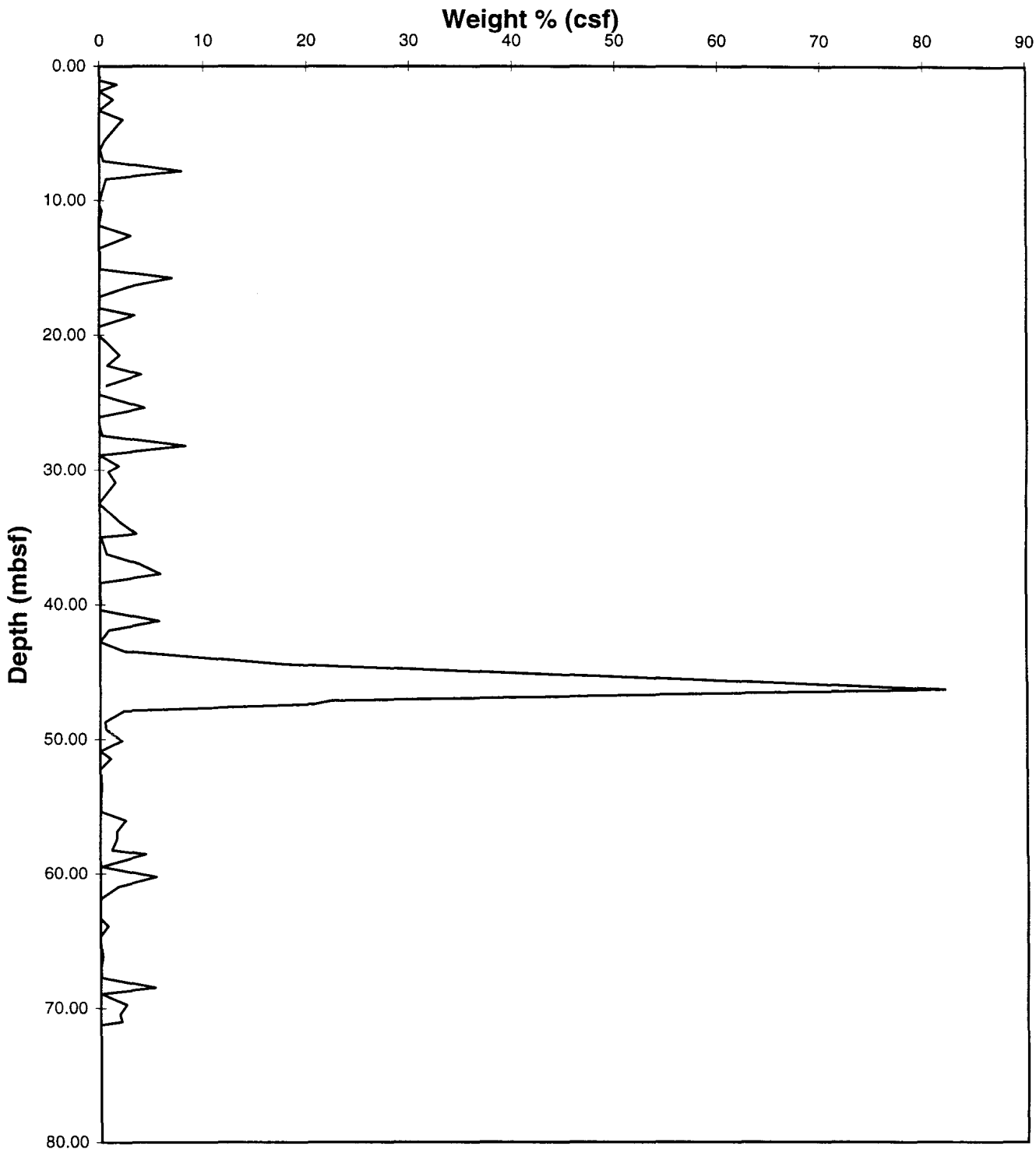
SITE 918
Weight % (csf)
0
10
20
30
40
50
60
70
80
90
Depth (mbsf)
0.00
10.00
20.00
30.00
40.00
50.00
60.00
70.00
80.00

Figure 4.

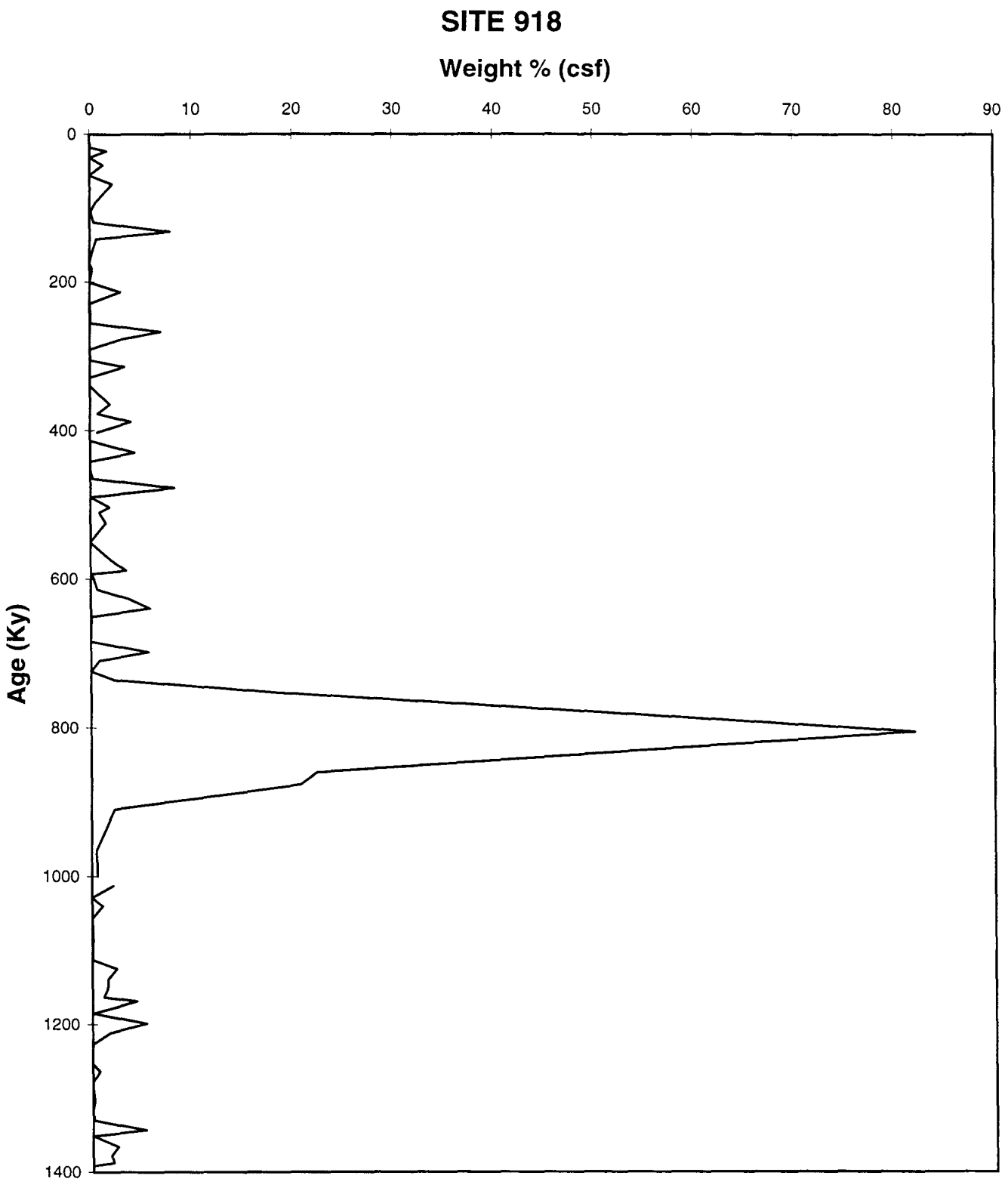
SITE 918
Weight % (csf)
0
10
20
30
40
50
60
70
80
90
Age (Ky)
0
200
400
600
800
1000
1200
1400

Figure 5.

Site 918

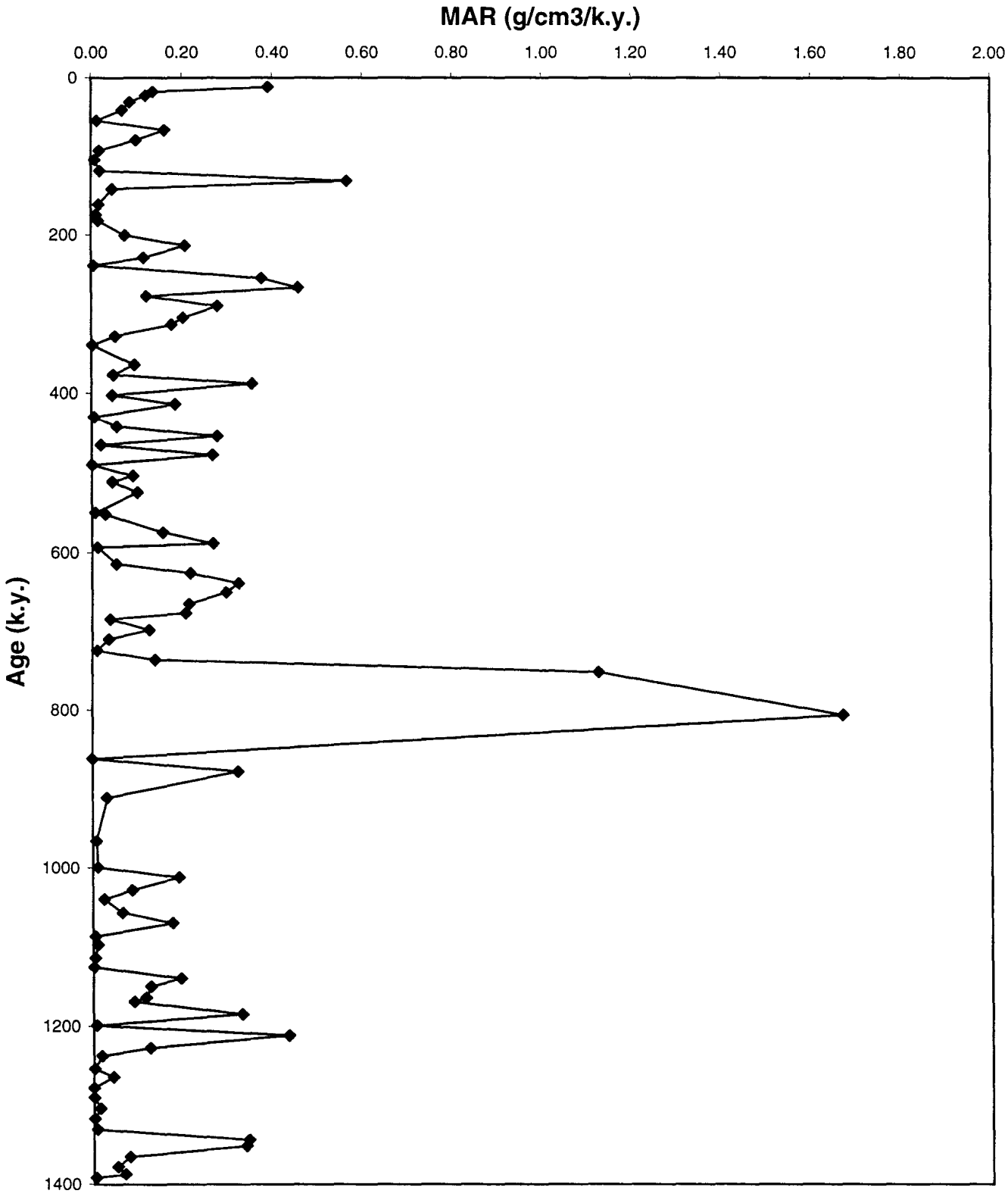

Figure 6.

Appendix

Wt % csf is the weight percent of the coarse-sand fraction of the total sample.

% IRD is the estimated abundance of ice-rafted debris within the coarse-sand fraction.

LSR is the linear sedimentation rate (cm/ k.y.).

Dry Bulk Density of the sediment for each sample (g/cm^3).

MAR is the mass accumulation rate of the IRD (g/cm^2 /k.y.).

					(cm)	(cm)	(mbsf)			(cm/ky)	(g/cm^3)	(g/cm^2/ky)	(ky)
											Dry Bulk		
Site	Hole	Core	Type	Section	Top	Bottom	Depth	CS wt%	% IRD	LSR	Density	MAR	Age
918	A	1	H	1	70	72	0.70000	8.56175	92	5.9	0.84	0.3904	11.864
918	A	1	H	2	5	7	1.05000	2.65752	70	5.9	1.24	0.1361	17.797
918	A	1	H	2	35	37	1.35000	1.67343	98	5.9	1.24	0.1200	22.881
918	A	2	H	1	5	7	1.85000	1.45853	87	5.9	1.14	0.0853	31.356
918	A	2	H	1	65	67	2.45000	1.32223	77	5.9	1.14	0.0685	41.525
918	A	2	H	1	145	147	3.25000	0.19410	99	5.9	1.14	0.0129	55.085
918	A	2	H	2	65	67	3.95000	2.25548	98	5.9	1.24	0.1617	66.949
918	A	2	H	2	142	144	4.72000	1.36692	99	5.9	1.24	0.0990	80.000
918	A	2	H	3	70	72	5.50000	0.54124	48	5.9	1.20	0.0184	93.220
918	A	2	H	3	140	142	6.20000	0.09683	92	5.9	1.74	0.0091	105.085
918	A	2	H	4	80	82	7.05000	0.42487	72	5.9	1.04	0.0188	119.492
918	A	2	H	5	5	7	7.80000	7.87849	95	5.9	1.28	0.5652	132.203
918	A	2	H	5	65	67	8.40000	0.65871	94	5.9	1.28	0.0468	142.373
918	A	2	H	6	28	30	9.53000	0.22438	82	5.9	1.60	0.0174	161.525
918	A	2	H	7	5	7	10.30000	0.24760	67	5.9	1.08	0.0106	174.576
918	A	2	H	7	50	52	10.75000	0.25345	98	5.9	1.08	0.0158	182.203
918	A	3	H	1	54	56	11.84000	0.90321	92	5.9	1.53	0.0750	200.678
918	A	3	H	2	64	66	12.59000	3.02445	99	5.9	1.17	0.2067	213.390
918	A	3	H	3	6	8	13.51000	1.81406	97	5.9	1.11	0.1152	228.983
918	A	3	H	3	64	66	14.09000	0.08622	98	5.9	1.11	0.0055	238.814
918	A	3	H	4	10	12	15.05000	5.81879	73	5.9	1.50	0.3759	255.085
918	A	3	H	4	79	81	15.74000	6.98127	74	5.9	1.50	0.4572	266.780
918	A	3	H	4	144	146	16.39000	2.83742	78	5.9	0.93	0.1214	277.797
918	A	3	H	5	69	71	17.14000	5.45570	88	5.9	0.98	0.2776	290.508
918	A	3	H	6	5	7	18.00000	3.26326	82	5.9	1.28	0.2021	305.085
918	A	3	H	6	58	60	18.53000	3.38354	69	5.9	1.28	0.1763	314.068
918	A	3	H	6	144	146	19.39000	1.07690	75	5.9	1.10	0.0524	328.644
918	A	3	H	7	60	62	20.05000	0.03442	75	5.9	1.42	0.0022	339.831
918	A	4	H	1	70	72	21.50000	1.94325	57	5.9	1.45	0.0948	364.407
918	A	4	H	1	145	147	22.25000	0.74500	72	5.9	1.54	0.0487	377.119
918	A	4	H	2	60	62	22.90000	4.02376	98	5.9	1.52	0.3536	388.136
918	A	4	H	2	144	146	23.74000	0.71243	72	5.9	1.52	0.0460	402.373

918	A	4	H	3	61	63	24.41000	2.45173	98	5.9	1.30	0.1843	413.729
918	A	4	H	4	7	9	25.37000	0.06906	96	5.9	1.60	0.0063	430.000
918	A	4	H	4	77	79	26.07000	0.60037	98	5.9	1.60	0.0555	441.864
918	A	4	H	5	5	7	26.80000	3.68566	97	5.9	1.31	0.2763	454.237
918	A	4	H	5	68	70	27.43000	0.27461	98	5.9	1.31	0.0208	464.915
918	A	4	H	5	144	146	28.19000	8.24417	45	5.9	1.22	0.2670	477.797
918	A	4	H	6	64	66	28.89000	0.01991	97	5.9	0.97	0.0011	489.661
918	A	4	H	6	144	146	29.69000	1.85991	85	5.9	0.97	0.0905	503.220
918	A	4	H	cc	15	17	30.13000	0.86176	75	5.9	1.19	0.0454	510.678
918	A	5	H	1	63	65	30.93000	1.53003	92	5.9	1.21	0.1005	524.237
918	A	5	H	2	6	8	32.40000	0.08068	98	5.9	1.54	0.0072	549.153
918	A	5	H	2	74	76	32.54000	0.34527	98	5.9	1.48	0.0295	551.525
918	A	5	H	3	6	8	33.90000	1.98859	98	5.9	1.36	0.1564	574.576
918	A	5	H	3	43	45	34.73000	3.47567	96	5.9	1.36	0.2677	588.644
918	A	5	H	4	19	21	34.99000	0.12828	98	5.9	1.63	0.0121	593.051
918	A	5	H	4	143	145	36.23000	0.64526	86	5.9	1.63	0.0534	614.068
918	A	5	H	5	64	66	36.94000	3.68699	75	5.9	1.33	0.2170	626.102
918	A	5	H	5	141	143	37.71000	5.79969	67	5.9	1.41	0.3233	639.153
918	A	5	H	6	59	61	38.39000	6.42600	82	5.9	0.95	0.2953	650.678
918	A	5	H	6	145	147	39.25000	2.98089	97	5.9	1.25	0.2132	665.254
918	A	5	H	cc	9	11	39.94000	2.47619	98	5.9	1.44	0.2062	676.949
918	A	6	H	1	58	60	40.38000	0.76857	98	5.9	0.90	0.0400	684.407
918	A	6	H	1	140	142	41.20000	5.64205	42	5.9	0.90	0.1258	698.305
918	A	6	H	2	59	61	41.89000	0.82914	83	5.9	0.90	0.0365	710.000
918	A	6	H	2	144	146	42.74000	0.21487	95	5.9	0.90	0.0108	724.407
918	A	6	H	3	64	66	43.44000	2.34530	92	5.9	1.09	0.1388	736.271
918	A	6	H	4	10	12	44.40000	17.77215	65	5.9	1.65	1.1246	752.542
918	A	6	H	5	50	52	46.30000	82.02521	87	1.5	1.56	1.6699	806.667
918	A	6	H	5	132	136	47.12000	20.66522	100	1.5	1.56	0.5230	861.333
918	A	6	H	6	6	8	47.36000	2.27474	87	1.5	1.19	0.0353	877.333
918	A	6	H	6	56	58	47.86000	0.47258	78	1.5	1.19	0.0066	910.667
918	A	6	H	6	138	140	48.68000	0.54761	98	1.5	1.19	0.0096	965.333
918	A	6	H	cc	8	10	49.19000		98	1.5	1.39	0.0000	999.333
918	A	7	H	1	79	81	50.09000	4.08091	72	4.9	1.32	0.1900	1012.245
918	A	7	H	2	8	10	50.88000	2.09486	63	4.9	1.34	0.0867	1028.367

918	A	7	H	2	64	66	51.44000	0.39019	97	4.9	1.34	0.0249	1039.796
918	A	7	H	2	147	149	52.27000	1.01588	98	4.9	1.34	0.0654	1056.735
918	A	7	H	3	62	64	52.92000	2.28189	98	4.9	1.60	0.1753	1070.000
918	A	7	H	3	145	147	53.75000	0.07623	98	4.9	1.38	0.0051	1086.939
918	A	7	H	4	64	66	54.44000	0.12310	97	5.7	1.52	0.0103	1097.018
918	A	7	H	5	8	10	55.38000	0.05888	98	5.7	1.57	0.0052	1113.509
918	A	7	H	5	74	76	56.04000	0.04175	75	5.7	1.57	0.0028	1125.088
918	A	7	H	6	7	9	56.87000	2.42786	97	5.7	1.44	0.1933	1139.649
918	A	7	H	6	64	66	57.44000	1.57860	98	5.7	1.44	0.1270	1149.649
918	A	7	H	6	144	146	58.24000	1.56967	90	5.7	1.44	0.1160	1163.684
918	A	7	H	cc	10	12	58.55000	1.13070	98	5.7	1.43	0.0903	1169.123
918	A	8	H	1	67	69	59.47000	4.36736	93	5.7	1.42	0.3287	1185.263
918	A	8	H	1	146	148	60.26000	0.09280	95	5.7	1.42	0.0071	1199.123
918	A	8	H	2	69	71	60.99000	5.33947	87	5.7	1.63	0.4316	1211.930
918	A	8	H	3	7	9	61.87000	1.70239	99	5.7	1.30	0.1249	1227.368
918	A	8	H	3	64	66	62.44000	0.25544	98	5.7	1.30	0.0185	1237.368
918	A	8	H	4	6	8	63.36000	0.03700	80	5.7	1.40	0.0024	1253.509
918	A	8	H	4	65	67	63.95000	0.73070	75	5.7	1.40	0.0437	1263.860
918	A	8	H	4	144	146	64.74000	0.01179	98	5.7	1.38	0.0009	1277.719
918	A	8	H	5	64	66	65.44000	0.04639	42	5.7	1.64	0.0018	1290.000
918	A	8	H	5	144	146	66.24000	0.21080	75	5.7	1.64	0.0148	1304.035
918	A	8	H	6	67	69	66.97000	0.02573	98	5.7	1.57	0.0023	1316.842
918	A	8	H	6	144	146	67.74000	0.10529	96	5.7	1.48	0.0085	1330.351
918	A	9	H	1	19	21	68.49000	5.23793	91	5.7	1.26	0.3423	1343.509
918	A	9	H	1	64	66	68.94000	5.44941	86	5.7	1.26	0.3366	1351.404
918	A	9	H	1	144	146	69.74000	2.49873	48	5.7	1.17	0.0800	1365.439
918	A	9	H	2	66	68	70.46000	1.82130	47	5.7	1.09	0.0532	1378.070
918	A	9	H	2	119	121	70.99000	2.04682	55	5.7	1.09	0.0699	1387.368
918	A	9	H	2	144	146	71.24000	0.09591	98	5.7	1.09	0.0058	1391.754